Arabian Journal of Chemistry (2023) **16**, 104477

King Saud University

Arabian Journal of Chemistry

www.ksu.edu.sa
www.sciencedirect.com

ORIGINAL ARTICLE

Gandouling alleviates cognitive dysfunction by regulates the p62/Nrf2 signaling pathway to reduce oxidative stress and autophagy in mice models of Wilson's disease

Zhangsheng Jiang [a], Ting Dong [b,*], Yan Wang [c], Lulu Tang [b], Chenling Zhao [a], Yuya Wen [a], Jie Chen [a]

[a] *Graduate School of Anhui University of Chinese Medicine, Hefei 230038, China*
[b] *The First Affiliated Hospital of Anhui University of Chinese Medicine, Hefei 230031, China*
[c] *College of Integrated Chinese and Western Medicine, Anhui University of Traditional Chinese Medicine, Hefei 230038, China*

Received 9 July 2022; accepted 28 November 2022
Available online 5 December 2022

KEYWORDS

GDL;
Wilson;
Cognitive;
Autophagy;
Nrf2;
p62

Abstract Cognitive impairment is a neurological manifestation of Wilson's disease (WD). Gandouling (GDL), a traditional Chinese medicine, protects against WD-related brain damage. However, the mechanisms underlying its protective effect have not been elucidated. Therefore, we explored the neuroprotective effects of GDL on cognitive abilities to understand the underlying molecular mechanisms using a toxic milk mouse model of WD. We employed the Morris water maze test and open field test to assess the effects of GDL on spatial memory, learning abilities and exploratory behavior in these mice. GDL treatment reduced the escape latency and increased the number of times mice crossed the platform to reach the target zone, indicative of alleviated WD-associated cognitive dysfunction. It also ameliorated the histopathological changes in the hippocampus via downregulation of IL-1β, IL-6, and TNF-α expression, reduced oxidative stress, and increased cell vigor. GDL treatment increased the protein and mRNA levels of Nrf2 and OH-1 protein while lowering p62, Beclin1, and LC3 expression in the hippocampus. Collectively, GDL improves cognitive dysfunction in mice with WD by regulating the Nrf2/p62 signaling path-

* Corresponding author.
E-mail address: dongting2002@sina.com (T. Dong).
Peer review under responsibility of King Saud University.

Production and hosting by Elsevier

https://doi.org/10.1016/j.arabjc.2022.104477

way by reducing oxidative stress and autophagy. Based on its anti-inflammatory, antioxidant, and autophagy-inhibiting effects, we believe GDL is a promising therapy for WD-related cognitive dysfunction.

1. Introduction

Wilson's disease (WD) is a recessive genetic disorder caused by aberrant copper metabolism. It is caused by a genetic defect in the ATPase copper transport β gene (*ATP7B*). Impaired copper excretion eventually leads to progressive pathological accumulation of copper in the liver, nervous system, and other tissues, resulting in damage to the brain, liver, kidney, and other related organs (Guindi, 2019). The risk of cognitive disorder in patients with WD has been affirmed and requires further attention (Wu et al., 2021; Shribman et al., 2022). Patients with neurological presentations lack fluid intelligence, a function of visual space, and have a lower processing rate than those with hepatic symptoms (Iwański et al., 2015; Wenisch et al., 2013). WD-related cognitive impairment can manifest as defects in learning, memory, reasoning, and speech expression. Recent studies have suggested that patients with neurological presentations have a poor memory for faces, and defects in facial expression recognition were relevant to an analogous schema of abnormalities with decreased grey matter volumes in the subcortex and medial prefrontal cortex regions (Shribman et al., 2022). An increase in the incidence of WD will increase the risk of dementia and the psychosocial burden on both families and society. Hence, early treatment to intervene in the progression of cognitive impairment to dementia in WD patients is critical. Nevertheless, given the lack of targeted therapies for WD-related cognitive impairment, there is an urgent need to develop new therapies.

The hippocampus and frontal cortex regions of the brain are involved in the formation, processing, consolidation, and retrieval of memory. These regions are highly susceptible to age-related oxidative stress and inflammation (Guo and Yang, 2020; Sawikr et al., 2017). Using mice models of WD, several studies have shown the involvement of neuroinflammation in WD-related cognitive impairment based on the levels of inflammatory cytokines such as interleukin (IL)-6, IL-1β, and tumor necrosis factor (TNF)-α in the hippocampus (Dong et al., 2021; Wu et al., 2019; Kalita et al., 2021). Moreover, the interplay among oxidative stress, inflammation, and regulation of autophagy plays a critical role in cognitive outcomes in the aging brain (Hensley and Harris-White, 2015).

Nrf2, a key endogenous regulator of various pathological and physiological events, is thought to be a central signaling molecule modulating autophagy, oxidative stress, and inflammation. It limits inflammation by suppressing reactive oxygen species (ROS) and inflammatory cytokines, such as IL-1β and IL-6 (Early et al., 2018; Yang and Chen, 2021). Autophagy regulates cell survival or death in different cell types and environments under various stress stimuli (Jin et al., 2012). Excess autophagy leads to cell dysfunction and death (Wang et al., 2022). Excessive accumulation of ROS induces oxidative stress and autophagy under pathological conditions such as ischemia/reperfusion or tumor hypoxia. Furthermore, autophagy can reduce oxidative damage by resolving or devouring oxidative substances (Zhou et al., 2022; Xu et al., 2021).

SQSTM-1/p62 is a multifunctional and multifaceted adapter protein whose primary function is to transport ubiquitinated proteins to the proteasome for degradation (Guo et al., 2021). Impaired peroxisomes lead to cellular accumulation of ROS, and dysfunctional peroxisomes are cleared by autophagy through pexophagy, a process closely related to p62 regulation (Wen et al., 2021). A recent study indicated substantially lower levels of Nrf2 in the hippocampus of mouse models of WD (Dong et al., 2021a). Treatment with ML385, an Nrf2 inhibitor, decreased the ratio of MAP2 + and Tuj1 + cells, blocking the differentiation of neural stem cells (NSCs) and exacerbating the cognitive decline in mice with WD. Inhibition of Nrf2 is perhaps connected with long-time high copper levels and oxidative stress in patients with WD. The loss or poor activation of Nrf2 aggravates oxidative stress, disrupting the normal cellular REDOX homeostasis and leading to cellular dysfunction and death (Mitsuishi et al., 2012). Several studies have reported excessive autophagy in cognitively impaired mice with WD. Zhang et al. observed an increased expression of LC3, an autophagy marker, in the hippocampus of mice with WD (Zhang et al., 2020). Inhibiting autophagy in these mice improved their cognitive function. Thus, underlying WD-related cognitive impairment may be excessive autophagy and lowered Nrf2 activation, contributing to oxidative stress and inflammation. Regulating the autophagy-Nrf2 axis may, therefore, be a crucial treatment strategy for WD-related cognitive impairment.

Gandouling (GDL) is a Chinese medicine granule prepared by the preparation center of Anhui Hospital of TCM. It is mainly composed of Rhizoma coptidis (Chinese name: Huanglian), Rhizoma zedoariae (Chinese name: Ezhu), Salvia miltiorrhiza (Chinese name: Danshen), Rheum officinale (Chinese name: Dahuang), Turmeric (Chinese name: Jianghuang), and Caulis spatholobi (Chinese name: Jixueteng). GDL and its components help in clearing heat, detoxification, removing blood stasis and dispersing knots, promoting gallbladder function, and discharging copper. GDL, combined with low-dose Penicillamine (Pen), has been shown to treat WD patients with neurological symptoms reliably and effectively (Zhang et al., 2018). Another study using a mouse model of WD showed that GDL with Pen improved brain injury through the PERK/eIF2α/CHOP stress pathway (Chen et al., 2018). However, its effects on autophagy and the p62/Nrf2 axis remain unclear.

Hence, in this study, we used the toxic milk mouse model for WD-related cognitive impairment to further elucidate the protective effects of GDL on WD-related cognitive impairment and the potential role of autophagy and the Nrf2/p62 pathway.

2. Materials and methods

2.1. Animals and grouping

Sixty SPF (Specific Pathogen Free) female toxic milk C3He-Atp7bTX-J/J (TX-J) mice were randomly divided into four groups: (1) control (including ten homologous wild-type healthy mice), (2) model (mice with WD), (3) GDL (WD mice treated with GDL alone), (4) Pen (WD mice treated with Pen alone). The animals were purchased from Jackson Laboratory and reared in the Animal Center of the Key Laboratory of the Ministry of Education, Anhui University of Traditional Chinese Medicine. The animals were kept in isolation cages with a separate air supply in a moisture controlled (40–60 %) environment at an indoor temperature of 25 ± 1 °C. They were provided sterile food and water. All animal protocols were approved by the Institutional Animal Care

and Use Committee of Anhui University of Chinese Medicine (Approval number: AHUCM-mouse-2021011).

2.2. Modeling and drug administration

Mice in the GDL group were administered GDL tablets of different strengths (GDL high, 1.16; GDL middle, 0.58; and GDL low, 0.29 g/kg per day) by gavage. GDL was produced by the Anhui Hospital of TCM (batch number: 20200726). Mice in the Pen group were given Pen (H31022286, Shanghai *sym*, China) tablets by gavage (0.1 g/kg per day). The treatment continued for six weeks. The stomachs of mice in the control and model groups were irrigated with similar volumes of distilled water.

2.3. Effect of GDL on WD-related cognitive impairment

2.3.1. Morris water maze test

After the sixth week of GDL administration, the spatial memory and learning ability of the TX-J mice were assessed using the Morris water maze (MWM) test. The experimental facility had a circular pond (60 cm in radius, 60 cm in height) filled with turbid water (40 cm in depth, 25 ± 1 °C). The pond was divided into four quadrants: northwest, northeast, southwest, and southeast. A lucent and transparent escape platform was placed between the northeast and southeast quadrants (target quadrant) 3 cm below the water surface. The mice were lightly placed in water in the quadrant opposite the target quadrant. During the training, the total swimming distance and time taken to escape (escape latency) using the platform were recorded for five consecutive days, 90 s each time. On the sixth day of the MWM test, the platform was moved to conduct a probe test, and the number of times the mice swam across the former location of the platform to reach the target quadrant was recorded for 90 s. During the experiment, rat behavior was recorded with MWM video tracking test system.

2.3.2. Open field test

In the circular mine, the bottom of the open field is divided into 25 grids, the four walls are peripheral grids, and the center is central grids. Mice were placed in the central grids, and the time of staying in the central grids, the number of crossing grids and the number of upright positions of mice were recorded within 3 min. After the test, wipe the bottom and surrounding area of the instrument with alcohol to eliminate odor interference.

2.3.3. Specimen collection and storage

Soon after the MWM test, model groups mice were anesthetized with 1 % pentobarbital sodium (40 mg/kg, given intraperitoneal injection) and mercy killing. The brain of three model groups mice were isolated and fixed in 4 % paraformaldehyde for H&E, Nissl, TUNEL and immunohistochemical staining. The cornu ammonis 1 (CA1) regions of hippocampal were cut into 1-mm^3 size samples and fixed in 2.5 % glutaraldehyde at 4 °C for transmission electron microscope (TEM) to observe. The hippocampus left behind were frozen in liquid nitrogen and stored at −80 °C for western blotting, Quantitative real-time polymerase chain reaction and ELISA.

2.3.4. H&E and Nissl staining

Brain tissue that had been fixed for more than 24 h was washed and then dehydrated in turn in a dehydrator with graded alcohol. The dehydrated brain tissue was embedded in paraffin and cut into 2-μm thick sections with a paraffin slicer. The histopathology changes of hippocampal CA1 and CA3 region were stained with H&E, and the functional changes of neurons were stained with 0.1 % toluidine blue for Nissl staining. The pictures were observed and analyzed under a microscope (BX51, OLYMPUS, JPN) at a magnification of 200× and 400×.

2.3.5. TUNEL staining

TUNEL staining was operated on paraffin sections of the brain samples using the in situ cell death detection kit (Intergen, USA) on the basis of the manufacturer's explanatory memorandum. After dewaxing and hydration, the protease K (20 μg/ml) was permeated for 20 min at indoor temperature. The slices were then placed in a mixture of TdT equilibrium buffer, recombinant TdT enzyme and Alexa Fluor 488–12-DUTP-labeled solution and reacted at 37 °C for 60 min. The nuclei were stained by DAPI method.

2.4. The mechanism of GDL on Wilson's disease-related cognitive impairment

2.4.1. Analysis of superoxide dismutase (SOD) and hippocampal glutathione (GSH) levels

The hippocampal samples were take out from refrigerator at −80 °C and these samples were prepared on the basis of the manufacturer's explanatory memorandum(Jiancheng Bioengineering Institute Co., Ltd., Nanjing, China). The content of GSH (A005-1)and SOD (A001-3) were detected.

2.4.2. ELISA of IL-1β, IL-6 and TNF-α in hippocampus

The IL-1β (JYM0531Mo), IL-6(JYM0012Mo) and TNF-α (JYM0218Mo) levels in hippocampus were detected by ELISA kits (Jiyinmei Technology Co., Ltd., Wuhan, China). All experimental steps were proceed according to the the manufacturer's explanatory memorandum.

2.4.3. Immunohistochemistry staining

The 2-μm tissue sections were deparaffinized in xylene and hydrated through graded ethanols. Staining was performed according to the staining procedure set by LC3 antibody, and the tablets were sealed. After EDTA(PH9.0) high pressure repair and air injection, the reaction time was 5 min-H_2O_2(3 %) at 37 °C for 10 min. LC3 antibody was incubated at 37 °C for 60 min and HRP was incubated at 37 °C for 30 min. Enhanced DAB color kit was used at 37 °C for 10 min to restain and seal tablets. At each step, wash with PBS + Tween 20 solution 3 times, 5 min each time.

2.4.4. Ultrastructural morphological observation by TEM

The tissue diameter of hippocampal CA1 region was modified to 1 mm^3 and fixed in 2.5 % glutaraldehyde for 1 h. Then the samples were treated with 1 % osmium tetroxide, dehydrated and embedded in Durcupan. The samples were cut into 60 nm slices and installed on Cu grids, and compared with ura-

nyl acetate and lead citrate. The ultrastructure of mitochondrion in the neurons was observed by TEM(FEI, Hillsboro, OR, USA).

2.4.5. Western blotting analysis

Hippocampal tissues of each group were collected in a −80 °C refrigerator, and homogenized in a grinding bead homogenizer. Protein lysate was added to extract total protein of skin tissue. BCA protein analysis kit (P0010S, Beyotime Institute of Biotechnology) was used. The proteins were separated by electrophoresis with 10 % SDS-PAGE gel for 70 min, transferred to PVDF membrane by wet method, and then sealed with 5 % milk at room temperature for 90 min, the blotted membranes were added with primary antibodies against Nrf2 (AF0639, Affinity, USA), OH-1(AF5393, Affinity, USA), Beclin-1 (ab207612, Abcam, UK), *p*62 (ab207305, Abcam, UK), LC3 (12741T, Cell Signaling, USA), α-tubulin(AF0001, Beyotime Biotechnology, China) during night at 4 °C. On the following day, after washing the membrane three times, the HRP-labeled goat anti-rabbit IgG (H + L) antibody (A0423, Beyotime Biotechnology) was added and incubated at room temperature for 2 h. Finally, ultrasensitive ECL chemiluminescent solution (D046-1, Bridgen, China) was applied, and placed into the chemiluminescence analyzer to analyze the strip resultsby Chem Studio 515 (Analytik Jena AG, Germany), and Image J 1.8.0 software scanned to obtain gray values for statistical analysis.

2.4.6. Quantitative real-time polymerase chain reaction

Total RNA was extracted from hippocampus using tissue homogenizers and TRIzol reagent (R0016, Beyotime Biotechnology, China). Using the cDNA was reversely transcribed by a reverse transcription kit (Enzy Artisan, Shanghai, China). The mRNA levels were quantified by PerfectStart Green qPCR SuperMix (EnzyArtisan, Shanghai, China) in LightCycler 480 real-time PCR system. Using GAPDH as internal reference, the mRNA relative expression of Nrf2, p62, ATG5, Beclin1 was determined by $2^{-\Delta\Delta Ct}$ method. The following primers were used:

Gapdh.
Forward: GTGTTCCTACCCCCAATGTG.
Reverse: GTCATTGAGAGCAATGCCAG.
Nrf2.
Forward:CAGCATAGAGCAGGACATGGAG.
Reverse:GAACAGCGGTAGTATCAGCCAG.
P62.
Forward:GCTCTTCGGAAGTCAGCAAACC.
Reverse:GCAGTTTCCCGACTCCATCTGT.
ATG5.
Forward:CTATATGTACTGCTTCATCCACTGG.
Reverse:GAGAGTAAAGCAAGTTGGAATTCG.
Beclin1.
Forward:GGAGGGGTCTAAGGCGTCCAG.
Reverse:TCTTGAAGCTCGTGTCCAGTTTCAG.

2.5. Statistical analysis

GraphPad Prism 8.0.1 (GraphPad Software Inc., San Diego, CA, USA) statistical software was used for statistical analysis. All results have been presented as mean ± standard deviation (SD). Statistical group analysis was performed using one-way analysis of variance (ANOVA). Results with a p-value < 0.05 were considered statistically significant.

3. Results

3.1. Effects of GDL on cognitive impairment in TX-J mice

3.1.1. Morris water maze test

During the acquired spatial learning and memory training, the mice in the control group exhibited a lower escape latency than those in the model group from days 2–5 (Fig. 1A and C). The escape latency varied significantly between the GDL and model groups from day 2 till the end of the collection phase on day 6. However, on day 6, despite the difference between the GDL-middle and High groups, no significant difference was observed between the GDL-low and model groups. model groups mice exhibited a decrease in memory recall and swam fewer times across the former platform to reach the target quadrant. Mice that received high-dose GDL demonstrated a significantly higher frequency of platform crossing than the control mice (Fig. 1B and D). At the same time, compared with control mice, the model group mice spent more time in the water maze, and the GDL-high group mice spent less time in the water maze than the model group mice (Fig. 1E). These results suggest that GDL can improve spatial learning and memory impairment in model mice.

3.1.2. Open field test

After six weeks of GDL administration, the cognitive function of mice was tested by open field test. Compared with those in the control group, the number of *trans*-lattices and upright times of the model group were significantly reduced. Moreover, the GDL groups were higher than those of the model group. The central grids stay of the model group was prolonged, and the GDL groups were shorter than those in the model group (Fig. 2). These results suggest that GDL can improve the autonomic activity and exploration ability of model mice.

3.2. Effects of GDL on brain histomorphology

After six weeks of GDL administration, its effects on neuronal morphology were assessed using H&E and Nissl staining. The arrangement of the hippocampal neurons in the control group was clear and regular (Fig. 3B, C, and G). The cells had evident nucleoli and intact nuclear membranes with no pyknosis. Compared with that in the control group, the model group mice had loosely arranged and disorganized neurons in the CA1 and CA3 regions of the hippocampus with cell body edema, vacuoles, degeneration and necrosis, and nuclei arranged irregularly, hyperchromatic, and pyknotic. In the GDL groups, these pathological changes in the hippocampus were significantly relieved. Nissl staining revealed abundant Nissl bodies in the CA1 and CA3 regions of the hippocampus (Fig. 3E, F, and H) in the control group, while they were fewer in the model group. GDL treatment led to an increase in Nissl bodies.

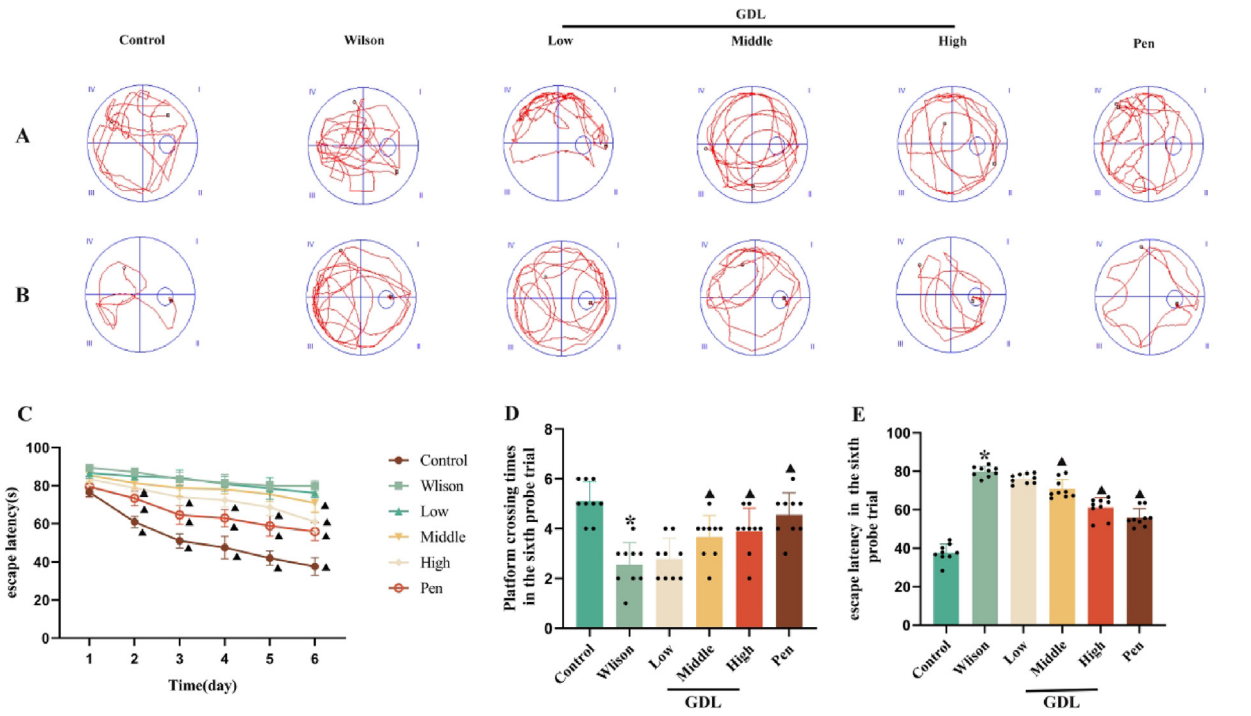

Fig. 1 Effects of GDL on spatial memory and learning in TX-J mice by used the MWM test. (A) The swimming trajectory of mice in each group in space exploration experiment. (B) The swimming traces of the acquisition training day 6. (C) The escape incubation period during six consecutive days. (D) Platform crossing times in the sixth probe trial. (E) Escape latency in the sixth probe trial. Statistical significance of all graphs was determined by one-way ANOVA. Data are presented as mean ± SD (n = 9); *$p < 0.05$ vs the control group; ▲$p < 0.05$ vs the Wilson group.

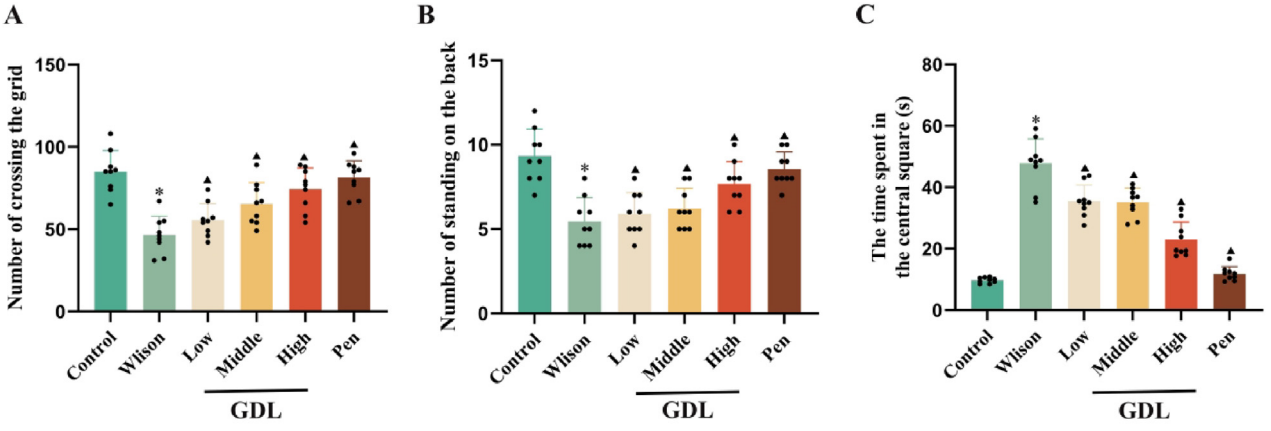

Fig. 2 Effects of GDL on exploratory behavior in TX-J mice by used the Open field test.(A)Number of crossing the grid. (B) Number of standing on the back. (C) The time apent in the central square. Statistical significance of all graphs was determined by one-way ANOVA. Data are presented as mean ± SD (n = 9); *$p < 0.05$ vs the control group; ▲$p < 0.05$ vs the Wilson group.

3.3. Effects of GDL on apoptosis in the frontal, temporal cortex

After six weeks of GDL administration, its effects on neuronal apoptosis in the frontal cortex of mice were examined by the TUNEL assay (Fig. 4). Apoptosis was significantly higher in the model group than in the control group. GDL treatment significantly reduced the rate of apoptosis in mice with WD.

3.4. Effects of GDL on hippocampal IL-1β, IL-6, TNF-α, GSH, and SOD levels

GDL intervention reduced IL-1β, IL-6, and TNF-α levels while increasing GSH and SOD levels in the hippocampus (Fig. 5), indicating the anti-inflammatory effects of GDL. It also appears to protect the hippocampal neurons from oxida-

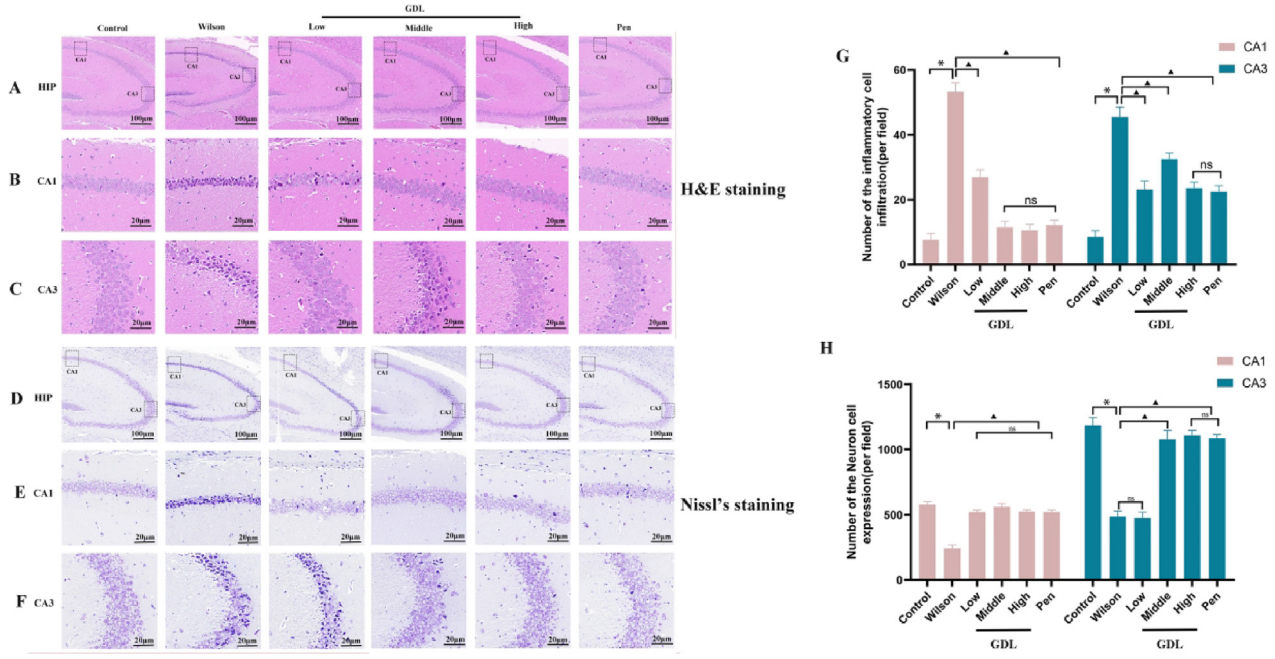

Fig. 3 Effects of GDL on brain injury and neuronal viability of TX-J mice. H&E-stained sections of hippocampal CA1 and CA3 regions (B, C and G); Nissl-stained neurons of the hippocampal CA1 and CA3 regions(E, F and H) of Sprague-Dawley mice visualized at 400×, Scale bar: 20 μm. Statistical significance of all graphs was determined by one-way ANOVA. Data are presented as mean ± SD (n = 6); *$p < 0.05$ vs the control group; ▲$p < 0.05$ vs the Wilson group.

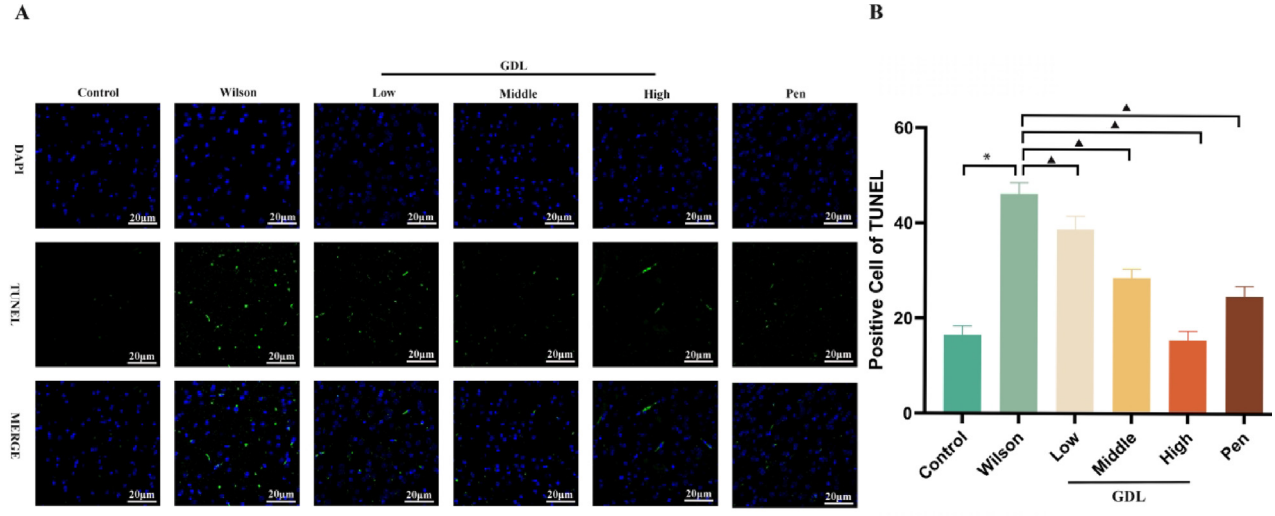

Fig. 4 Effect of GDL on apoptosis of frontal temporal cortex. TUNEL stained sections of frontal temporal cortex(A) of Sprague-Dawley mice visualized at 400×, Scale bar: 20 μm. Statistical significance of all graphs was determined by one-way ANOVA. Data are presented as mean ± SD (n = 6); *$p < 0.05$ vs the control group; ▲$p < 0.05$ vs the Wilson group.

tion, which could contribute to reversing the cognitive impairment caused by WD.

3.5. Effects of GDL on the ultrastructure of neurons

We examined the mitochondrial ultrastructure in all mice by TEM(Fig. 6). While the control group had healthy mitochondria, the model group had severely damaged mitochondria. The hippocampus of model group mice showed obscure mitochondrial fissures, high density swelling, mitochondria with decreased electron density, and fewer degenerated synaptic vesicles. However, GDL treatment improved the damage to hippocampal mitochondria.

3.6. Effect of GDL on the autophagy/Nrf2/p62 signaling pathway

We evaluated the levels of autophagy and Nrf2 expression by western blotting, qRT-PCR, and immunohistochemistry. Compared with the control group, the model group had

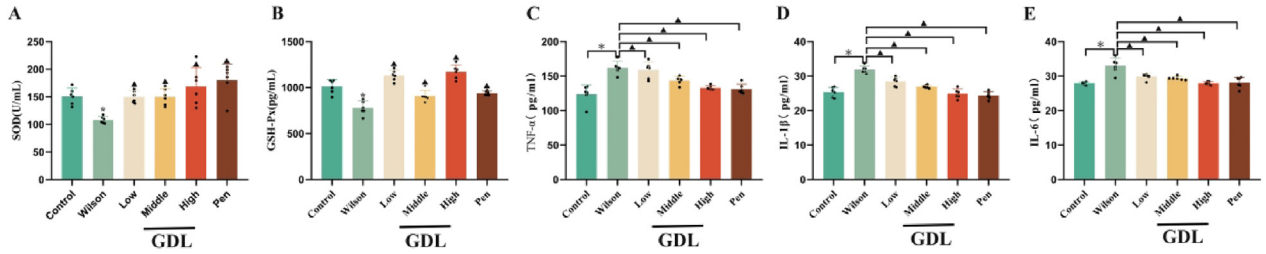

Fig. 5 Effects of GDL on hippocampal SOD (A), GSH (B), TNF-α (C), IL-1β (D) and IL-6 (E). Analytical results of (A), (B), (C), (D), and (E) using one-way ANOVA followed by Bonferroni's post hoc analysis. Statistical significance of all graphs was determined by one-way ANOVA. Data are presented as mean ± SD (n = 6); *$p < 0.05$ vs the control group;▲$p < 0.05$ vs the Wilson group.

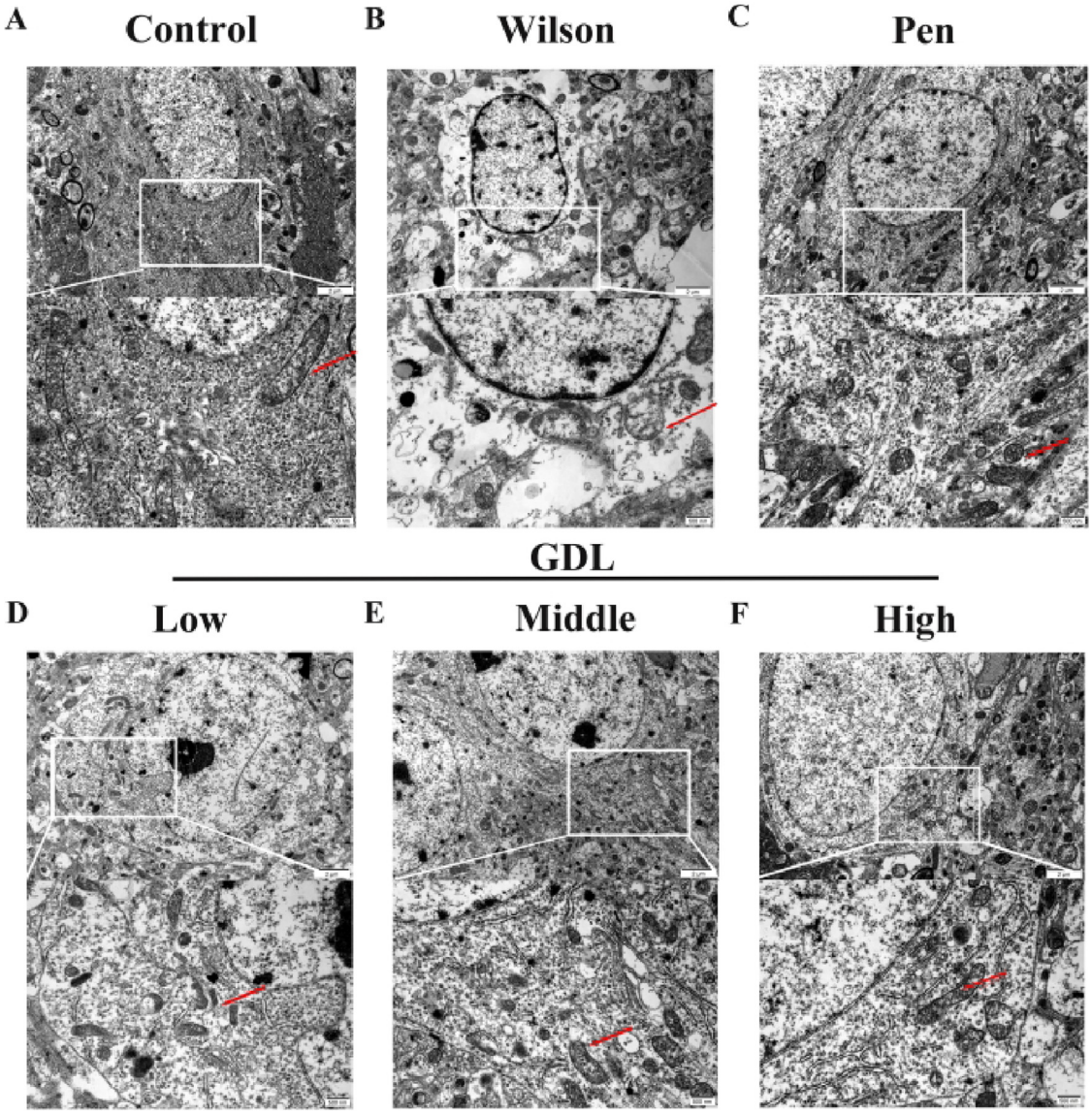

Fig. 6 Effects of GDL on ultrastructural synaptic changes in the hippocampus. (A) Healthy synapses, abundant synaptic vesicles and normal mitochondria in synapses (red arrowheads); (B) severe synaptic damage in the Wilson group: fuzzy synaptic cleft and relatively abundant synaptic vesicles, high electron density swelling and degeneration of mitochondria in synapses (red arrowheads, low electron density changes in partial synapses; (C) in the Pen group and (D, E and F) in the GDL group: the degree of synaptic damage above was reduced (scale bar = 2 μm and 500 nm).

reduced protein and mRNA levels of Nrf2 and OH-1 proteins but higher levels of autophagy-related proteins, Beclin1, p62, and LC3. The mRNA levels of Beclin1, p62, and ATG5 were also enhanced in the model group. However, GDL treatment lowered the expression of LC3, ATG5, p62, and Beclin1 while increasing the expression of Nrf2 and OH-1 compared to the model group (Fig. 7). Consistent with western blotting, immunohistochemistry also showed markedly elevated LC3 staining in the model group, which was reversed following GDL treatment (Fig. 8). Our results suggest that Nrf2 activa-

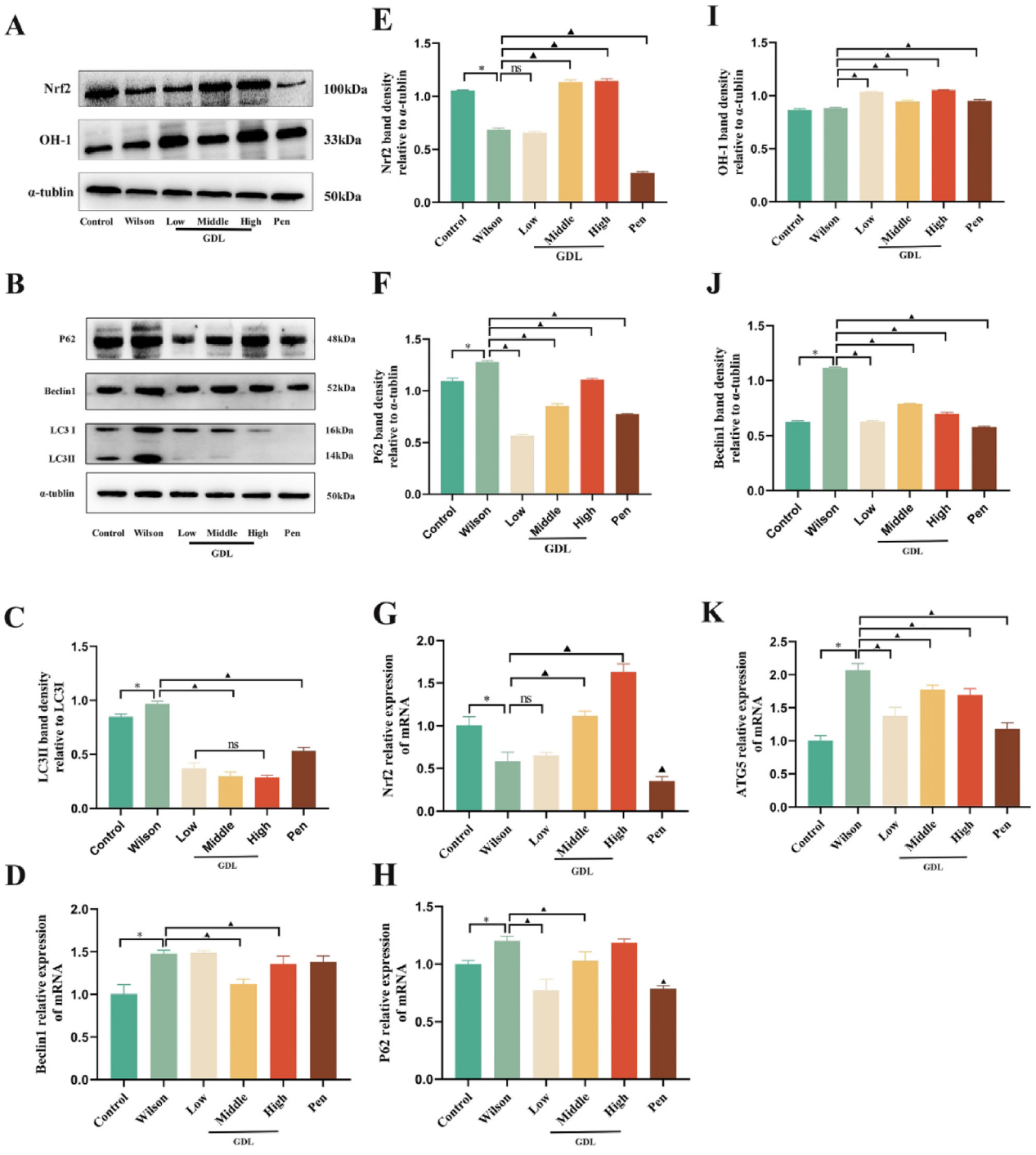

Fig. 7 Effects of GDL regulates the autophagy/Nrf2/p62 signaling pathway in the hippocampus of Wilson's disease-related cognitive impairment mice. (A–B and C, E, F, I J). Representative western blots of Nrf2, OH-1, Beclin1, *P*62, and LC3 in the hippocampus(n = 3 per group). Representative qRT-PCRs of Nrf2, *P*62, ATG5, Beclin1 in the hippocampus (n = 9 per group). Statistical significance of all graphs was determined by one-way ANOVA. Data are presented as mean ± SD (n = 9); *$p < 0.05$ vs the control group; ▲$p < 0.05$ vs the Wilson group.

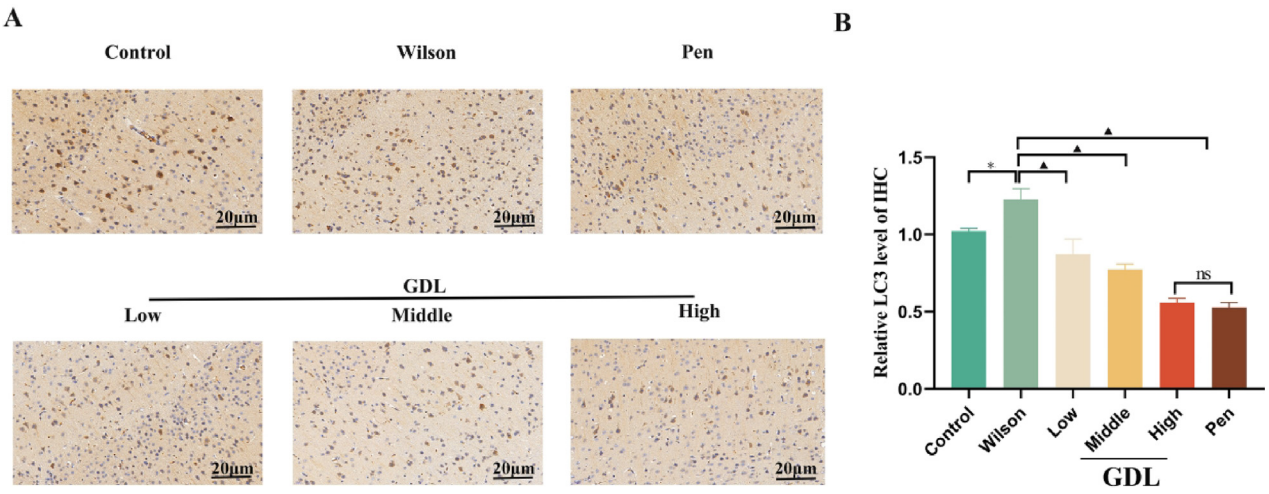

Fig. 8 Effects of GDL on the protein levels of LC3 in the hippocampus of Wilson's disease-related cognitive impairment mice. Representative microphotographs of immunofluorescence staining visualized at 400×, Scale bar: 20 μm; average optical density of LC3. Statistical significance of all graphs was determined by one-way ANOVA. Data are presented as mean ± SD (n = 3); *$p < 0.05$ vs the control group; ▲$p < 0.05$ vs the Wilson group.

tion and inhibition of p62 could be the mechanisms underlying GDL-mediated inhibition of autophagy in WD-related cognitively impaired mice.

4. Discussion

WD-related cognitive impairment can potentially lead to dementia, seriously affecting the patient's quality of life. However, we lack comprehensive insights into the mechanisms underlying WD-related cognitive impairment. Understanding the pathogenesis of cognitive impairment in WD will be beneficial in developing better therapies to improve the long-term prognosis. In this study, we observed excessive autophagy and Nrf2 suppression in the hippocampus of cognitively impaired mice with WD, consistent with previous findings (Dong et al., 2021a; Zhang et al., 2020). However, GDL intervention led to an inhibition of autophagy, activation of Nrf2, and alleviation of nerve inflammation, reducing oxidative stress and improved cognitive damage in these mice. To the best of our knowledge, this is the first study to demonstrate GDL-mediated inhibition of autophagy and regulation of Nrf2 in the hippocampus, providing a new therapeutic strategy to improve WD-related cognitive impairment in mice.

Recent studies have demonstrated Nrf2 inhibition in rodent models of Parkinson's and Alzheimer's diseases (Yang et al., 2020; Qu et al., 2020). WD is characterized by increased ROS production induced by long-term high copper levels leading to immune cell activation, Nrf2 inhibition, and increased IL-1β secretion, resulting in neuroinflammation and cognitive dysfunction (Lu et al., 2022; Dong et al., 2021). Chronic neuroinflammation is accompanied by neutrophil infiltration and microglial activation, leading to neuronal death and cognitive decline (Posillico et al., 2021; Breach et al., 2021). Anti-neuroinflammatory therapies have been used to treat WD-related cognitive impairment (Dong et al., 2021a; Dong et al., 2021b). In addition, Nrf2 activation provides neuroprotection during the pathological process by binding to the IL-1β promoter and suppressing its transcription, independent of ROS (Kobayashi et al., 2016). In our study, GDL effectively activated Nrf2 and inhibited the secretion of inflammatory cytokines, thereby improving WD-related cognitive impairment.

The Nrf2/p62 signaling pathway has become a research hotspot, given its vital role in cell defense and interaction with apoptosis, autophagy, and other signaling pathways (Peng et al., 2022). Expression of p62 is induced in cells under oxidative stress, resulting in a positive feedback loop by inducing transcription driven by antioxidant response elements (Choi et al., 2020).

Autophagy regulates various signaling pathways associated with pyroptosis, especially those related to oxidative stress. It has been shown to improve realgar-induced liver injury by inhibiting ROS-mediated activation of NLRP3 inflammasome (Yang et al., 2022). Inhibition of autophagy blocks the fusion of the autophagosome with the lysosome, leading to p62 accumulation (Klionsky et al., 2012). Neuroprotective effects of Xiao-xu-ming decoction have been reported in a rat model of CIR, Cerebral Ischemia and Reperfusion, improving the cognitive function of rats via downregulation of LC3, Beclin1, and mitochondrial p62 expression and inhibition of mitophagy (Lan et al., 2018). In this study, while significantly higher levels of LC3II/LC3I indicated increased autophagosome formation, higher levels of p62 highlighted the aberrant autophagy pathway in WD mice. GDL treatment significantly lowered p62 levels, suggesting that reversing autophagy defects may be one of the mechanisms by which GDL protects cells from oxidative stress-induced autophagy to improve cognitive function in mice.

We used a WD mouse model to verify the relationship between oxidative stress, autophagy, and Nrf2/p62 signaling pathway. These mice exhibited elevated levels of autophagy, oxidative stress, and p62, along with Nrf2 inhibition. Cytological studies have indicated that the hippocampal head is mainly folded by the CA1 area, which is the most sensitive to hypoxia-induced damage and is strongly associated with cognitive impairment (Aery Jones et al., 2021). Examination of hip-

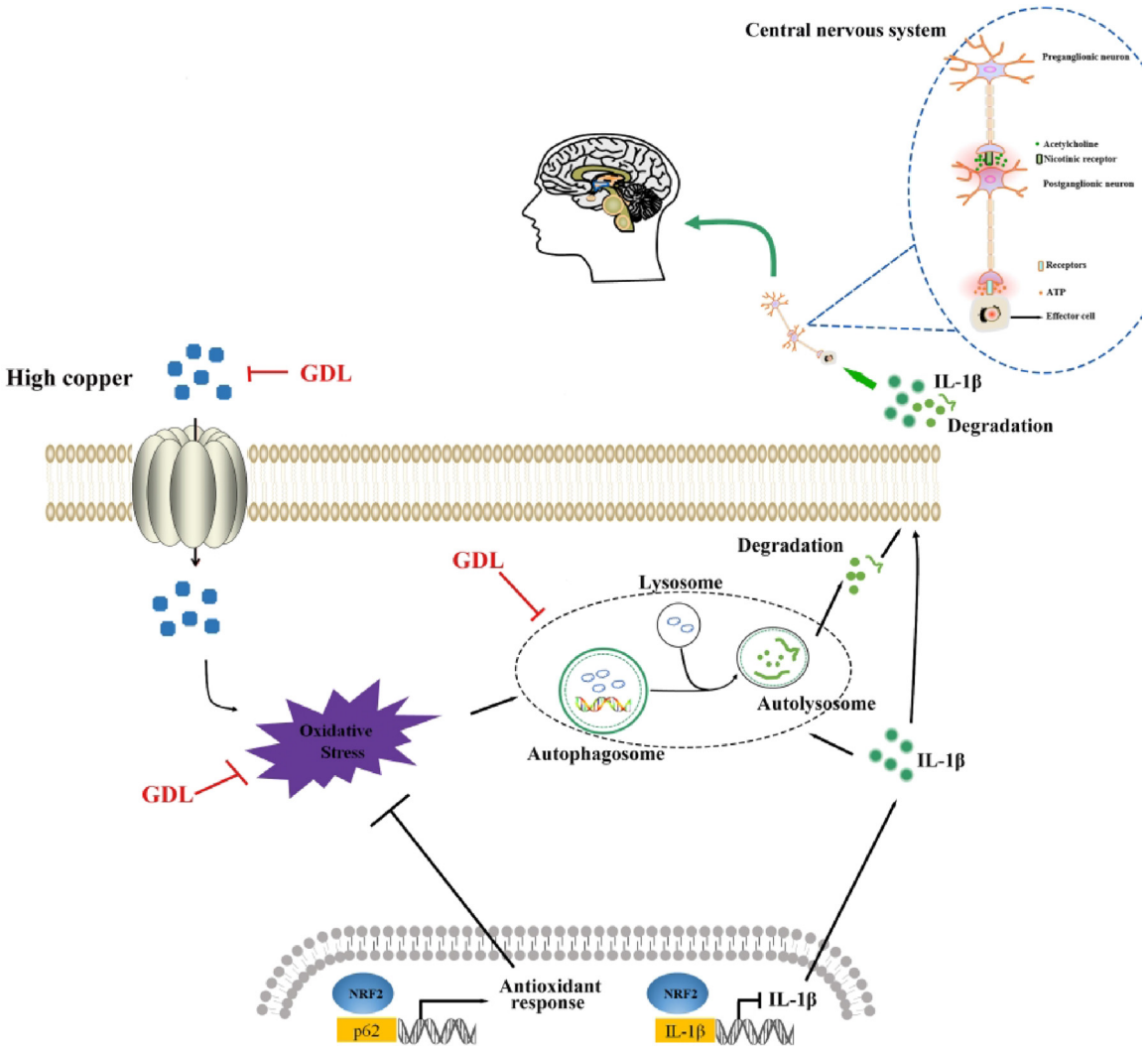

Fig. 9 Mechanism of GDL ameliorating Wilson's disease-related cognitive impairment. GDL inhibits autophagy, IL1β and enhances Nrf2 activation thereby repaired cognitive function. GDL also enhances the capacity of antioxidant enzymes.

pocampal CA1 mitochondria by TEM showed multiple mitochondria with decreased electron density, obscure mitochondrial fissures, high density swelling, and fewer and degenerated synaptic organelles. However, GDL treatment reversed the damage to the hippocampal mitochondria. We speculated that the therapeutic effect of GDL was closely related to its ability to induce Nrf2 activation and inhibit p62 expression and autophagy. However, it is still unclear if GDL directly affects the Nrf2 pathway and intracerebral autophagy or if the observed changes indirectly result from the improved neural antioxidant activity. Further studies are required to clarify these issues.

5. Conclusions

We confirmed higher oxidative stress, inflammation, and autophagy, along with Nrf2 inhibition in cognitively impaired mice with WD. GDL treatment of these mice resulted in Nrf2 activation accompanied by inhibition of autophagy and lower levels of IL-1β family cytokines, potentially related to the inhibition of IL-b transcription by Nrf2 (Fig. 9). We believe these effects of GDL on Nrf2/p62 signaling contributed to its ability to improve cognitive impairment in the treated mice. Our results support the clinical application of GDL to treatment strategies for WD. However, further in vivo and in vitro studies are required to elucidate the exact mechanisms of autophagy and oxidative stress in WD.

Declaration of Competing Interest

The authors declare that they have no known competing financial interests or personal relationships that could have appeared to influence the work reported in this paper.

Acknowledgments

The authors would like to express their gratitude to the Specialized Research Fund for Natural Science Foundation of Anhui Province (No.2108085QH366); the Natural Science Foundation of Anhui Province (2208085MH270); the Clinical Research Project of the First Affiliated Hospital of Anhui University of Traditional Chinese Medicine (No.2020Y-FYZC01); the Science and Technology Innovation Fund of Anhui University of Traditional Chinese Medicine (No.2021ZC08); the Natural Science Research Project of

Anhui Universities (No. KJ2021A0547); and the Graduate Scientific Research Project of Anhui Universities (No. YJS20210476).

References

Aery Jones, E.A., Rao, A., Zilberter, M., Djukic, B., Bant, J.S., Gillespie, A.K., Koutsodendris, N., Nelson, M., Yoon, S.Y., Huang, K., Yuan, H., Gill, T.M., Huang, Y., Frank, L.M., 2021. Dentate gyrus and CA3 GABAergic interneurons bidirectionally modulate signatures of internal and external drive to CA1. Cell Rep. 37, (13) 110159.

Breach, M.R., Dye, C.N., Joshi, A., Platko, S., Gilfarb, R.A., Krug, A. R., Franceschelli, D.V., Galan, A., Dodson, C.M., Lenz, K.M., 2021. Maternal allergic inflammation in rats impacts the offspring perinatal neuroimmune milieu and the development of social play, locomotor behavior, and cognitive flexibility. Brain Behav. Immun. 95, 269–286.

Chen, Y., Zhang, B., Cao, S., Huang, W., Liu, N., Yang, W., 2018. GanDouLing combined with Penicillamine improves cerebrovascular injury via PERK/eIF2α/CHOP endoplasmic reticulum stress pathway in the mouse model of Wilson's disease. Bioscience Reports 38 (5). BSR20180800.

Choi, Y., Jiang, Z., Shin, W.J., Jung, J.U., 2020. Severe Fever with Thrombocytopenia Syndrome Virus NSs Interacts with TRIM21 To Activate the p62-Keap1-Nrf2 Pathway. J. Virol. 94 (6), e01684–e10719.

Dong, J., Wang, X., Xu, C., Gao, M., Wang, S., Zhang, J., Tong, H., Wang, L., Han, Y., Cheng, N., Han, Y., 2021b. Inhibiting NLRP3 inflammasome activation prevents copper-induced neuropathology in a murine model of Wilson's disease. Cell Death Dis. 12 (1), 87.

Dong, T., Wu, M.C., Tang, L.L., Jiang, H.L., Zhou, P., Kuang, C.J., Tian, L.W., Yang, W.M., 2021a. GanDouLing promotes proliferation and differentiation of neural stem cells in the mouse model of Wilson's disease. Bioscience Reports 41 (1). BSR20202717.

Early, J.O., Menon, D., Wyse, C.A., Cervantes-Silva, M.P., Zaslona, Z., Carroll, R.G., Palsson-McDermott, E.M., Angiari, S., Ryan, D. G., Corcoran, S.E., Timmons, G., Geiger, S.S., Fitzpatrick, D.J., O'Connell, D., Xavier, R.J., Hokamp, K., O'Neill, L., Curtis, A. M., 2018. Circadian clock protein BMAL1 regulates IL-1β in macrophages via NRF2. PNAS 115 (36), E8460–E8468.

Guindi, M., 2019. Wilson disease. Semin Diagn Pathol. 36 (6), 415–422.

Guo, D., Yang, J., 2020. Interplay of the long axis of the hippocampus and ventromedial prefrontal cortex in schema-related memory retrieval. Hippocampus 30 (3), 263–277.

Guo, C., Zhang, Y., Nie, Q., Cao, D., Wang, X., Wan, X., Liu, M., Cui, J., Sun, J., Bai, Y., Li, L., 2021. SQSTM1/ p62 oligomerization contributes to Aβ-induced inhibition of Nrf2 signaling. Neurobiol. Aging 98, 10–20.

Hensley, K., Harris-White, M.E., 2015. Redox regulation of autophagy in healthy brain and neurodegeneration. Neurobiol. Dis. 84, 50–59.

Iwański, S., Seniów, J., Leśniak, M., Litwin, T., Członkowska, A., 2015. Diverse attention deficits in patients with neurologically symptomatic and asymptomatic Wilson's disease. Neuropsychology 29 (1), 25–30.

Jin, Y., Tanaka, A., Choi, A.M., Ryter, S.W., 2012. Autophagic proteins: new facets of the oxygen paradox. Autophagy 8 (3), 426–428.

Kalita, J., Kumar, V., Misra, U.K., Kumar, S., 2021. Movement Disorder in Wilson Disease: Correlation with MRI and Biomarkers of Cell Injury. J. Mol. Neurosci. : MN 71 (2), 338–346.

Klionsky, D.J., Abdalla, F.C., Abeliovich, H., Abraham, R.T., Acevedo-Arozena, A., Adeli, K., Agholme, L., Agnello, M., Agostinis, P., Aguirre-Ghiso, J.A., Ahn, H.J., Ait-Mohamed, O., Ait-Si-Ali, S., Akematsu, T., Akira, S., Al-Younes, H.M., Al-Zeer, M.A., Albert, M.L., Albin, R.L., Alegre-Abarrategui, J., Zuckerbraun, B., 2012. Guidelines for the use and interpretation of assays for monitoring autophagy. Autophagy 8 (4), 445–544.

Kobayashi, E.H., Suzuki, T., Funayama, R., Nagashima, T., Hayashi, M., Sekine, H., Tanaka, N., Moriguchi, T., Motohashi, H., Nakayama, K., Yamamoto, M., 2016. Nrf2 suppresses macrophage inflammatory response by blocking proinflammatory cytokine transcription. Nat. Commun. 7, 11624.

Lan, R., Zhang, Y., Wu, T., Ma, Y.Z., Wang, B.Q., Zheng, H.Z., Li, Y.N., Wang, Y., Gu, C.Q., Wu, J.T., 2018. Xiao-Xu-Ming Decoction Reduced Mitophagy Activation and Improved Mitochondrial Function in Cerebral Ischemia and Reperfusion Injury. Behav. Neurol. 2018, 4147502.

Lu, Q., Zhang, Y., Zhao, C., Zhang, H., Pu, Y., Yin, L., 2022. Copper induces oxidative stress and apoptosis of hippocampal neuron via pCREB/BDNF/ and Nrf2/HO-1/NQO1 pathway. J. Appl. Toxicol. 42 (4), 694–705.

Mitsuishi, Y., Motohashi, H., Yamamoto, M., 2012. The Keap1-Nrf2 system in cancers: stress response and anabolic metabolism. Front. Oncol. 2, 200.

Peng, L., Lu, Y., Zhong, J., Ke, Y., Li, Y., Liang, B., Li, H., Zhu, H., Li, Z., 2022. Lycium barbarum polysaccharide promotes proliferation of human melanocytes via activating the Nrf2/p62 signaling pathway by inducing autophagy in vitro. J. Food Biochem. 46 (10), e14301.

Posillico, C.K., Garcia-Hernandez, R.E., Tronson, N.C., 2021. Sex differences and similarities in the neuroimmune response to central administration of poly I:C. J. Neuroinflammation 18 (1), 193.

Qu, Z., Sun, J., Zhang, W., Yu, J., Zhuang, C., 2020. Transcription factor NRF2 as a promising therapeutic target for Alzheimer's disease. Free Radic. Biol. Med. 159, 87–102.

Sawikr, Y., Yarla, N.S., Peluso, I., Kamal, M.A., Aliev, G., Bishayee, A., 2017. Neuroinflammation in Alzheimer's Disease: The Preventive and Therapeutic Potential of Polyphenolic Nutraceuticals. Adv. Protein Chem. Struct. Biol. 108, 33–57.

Shribman, S., Bocchetta, M., Sudre, C.H., Acosta-Cabronero, J., Burrows, M., Cook, P., Thomas, D.L., Gillett, G.T., Tsochatzis, E. A., Bandmann, O., Rohrer, J.D., Warner, T.T., 2022a. Neuroimaging correlates of brain injury in Wilson's disease: a multimodal, whole-brain MRI study. Brain J. Neurol. 145 (1), 263–275.

Shribman, S., Burrows, M., Convery, R., Bocchetta, M., Sudre, C.H., Acosta-Cabronero, J., Thomas, D.L., Gillett, G.T., Tsochatzis, E. A., Bandmann, O., Rohrer, J.D., Warner, T.T., 2022b. Neuroimaging Correlates of Cognitive Deficits in Wilson's Disease. Movement Disorders : Off. J. Movement Disorder Soc. https://doi.org/10.1002/mds.29123.

Wang, C., Haas, M., Yeo, S.K., Sebti, S., Fernández, Á.F., Zou, Z., Levine, B., Guan, J.L., 2022. Enhanced autophagy in Becn1F121A/F121A knockin mice counteracts aging-related neural stem cell exhaustion and dysfunction. Autophagy 18 (2), 409–422.

Wen, W., Li, X., Yin, M., Wang, H., Qin, L., Li, H., Liu, W., Zhao, Z., Zhao, Q., Chen, H., Hu, J., Qian, P., 2021. Selective autophagy receptor SQSTM1/ p62 inhibits Seneca Valley virus replication by targeting viral VP1 and VP3. Autophagy 17 (11), 3763–3775.

Wenisch, E., De Tassigny, A., Trocello, J.M., Beretti, J., Girardot-Tinant, N., Woimant, F., 2013. Cognitive profile in Wilson's disease: a case series of 31 patients. Rev. Neurol. 169 (12), 944–949.

Wu, P., Dong, J., Cheng, N., Yang, R., Han, Y., Han, Y., 2019. Inflammatory cytokines expression in Wilson's disease. Neurol. Sci.: Off. J. Italian Neurol. Soc. Italian Soc. Clin. Neurophysiol. 40 (5), 1059–1066.

Wu, Y., Hu, S., Wang, Y., Dong, T., Wu, H., Zhang, Y., Qu, Q., Wang, A., Yang, Y., Li, C., Kan, H., 2021. The degeneration changes of basal forebrain are associated with prospective memory impairment in patients with Wilson's disease. Brain Behav. 11 (8), e2239.

Xu, Y., Ji, Y., Li, X., Ding, J., Chen, L., Huang, Y., Wei, W., 2021. URI1 suppresses irradiation-induced reactive oxygen species (ROS)

by activating autophagy in hepatocellular carcinoma cells. Int. J. Biol. Sci. 17 (12), 3091–3103.

Yang, F., Chen, R., 2021. Sestrin1 exerts a cytoprotective role against oxygen-glucose deprivation/reoxygenation-induced neuronal injury by potentiating Nrf2 activation via the modulation of Keap1. Brain Res. 1750, 147165.

Yang, Y., Kong, F., Ding, Q., Cai, Y., Hao, Y., Tang, B., 2020. Bruceine D elevates Nrf2 activation to restrain Parkinson's disease in mice through suppressing oxidative stress and inflammatory response. Biochem. Biophys. Res. Commun. 526 (4), 1013–1020.

Yang, J., Li, J., Guo, H., Zhang, Y., Guo, Z., Liu, Y., Huo, T., 2022. An Experimental Study Reveals the Protective Effect of Autophagy against Realgar-Induced Liver Injury via Suppressing ROS-Mediated NLRP3 Inflammasome Pathway. Int. J. Mol. Sci. 23 (10), 5697.

Zhang, J., Li, L., Chen, H., Yang, W., 2018. Clinical efficacy and safety of Gandouling plus low-dose D-penicillamine for treatment of Wilson's disease with neurological symptoms. J. Traditional Chinese Med. = Chung i tsa chih ying wen pan 38 (1), 89–94.

Zhang, J., Tang, L.L., Li, L.Y., Cui, S.W., Jin, S., Chen, H.Z., Yang, W.M., Xie, D.J., Yu, G.R., 2020. Gandouling Tablets Inhibit Excessive Mitophagy in Toxic Milk (TX-J) Model Mouse of Wilson Disease via Pink1/Parkin Pathway. Evid. Based Complement. Alternat. Med. 2020, 3183714.

Zhou, J., Li, X.Y., Liu, Y.J., Feng, J., Wu, Y., Shen, H.M., Lu, G.D., 2022. Full-coverage regulations of autophagy by ROS: from induction to maturation. Autophagy 18 (6), 1240–1255.